Microstructural and mechanical characterization of Zr modified 2014 aluminium alloy

P.Cavaliere

Department of "Ingegneria dell'Innovazione",

Engineering Faculty

Via per Arnesano

University of Lecce , I-73100 Lecce

Report Documentation Page

Form Approved
OMB No. 0704-0188

1. REPORT DATE	2. REPORT TYPE	3. DATES COVERED
18 MAR 2004	**N/A**	**-**

4. TITLE AND SUBTITLE	5a. CONTRACT NUMBER
Microstructural and mechanical characterization of Zr modified 2014 aluminium alloy	5b. GRANT NUMBER
	5c. PROGRAM ELEMENT NUMBER
6. AUTHOR(S)	5d. PROJECT NUMBER
	5e. TASK NUMBER
	5f. WORK UNIT NUMBER
7. PERFORMING ORGANIZATION NAME(S) AND ADDRESS(ES) **University of Lecce , Italy**	8. PERFORMING ORGANIZATION REPORT NUMBER
9. SPONSORING/MONITORING AGENCY NAME(S) AND ADDRESS(ES)	10. SPONSOR/MONITOR'S ACRONYM(S)
	11. SPONSOR/MONITOR'S REPORT NUMBER(S)

12. DISTRIBUTION/AVAILABILITY STATEMENT
Approved for public release, distribution unlimited

13. SUPPLEMENTARY NOTES
See also ADM001672., The original document contains color images.

14. ABSTRACT

15. SUBJECT TERMS

16. SECURITY CLASSIFICATION OF:			17. LIMITATION OF ABSTRACT	18. NUMBER OF PAGES	19a. NAME OF RESPONSIBLE PERSON
a. REPORT	b. ABSTRACT	c. THIS PAGE			
NATO/unclassified	**unclassified**	**unclassified**	**UU**	**47**	

Summary

-AA Zr modified 2014 aluminium alloy Optical and TEM observations

-Warm torsion tests

-Fatigue tests

-Fracture observations

Introduction

-Aluminium sheets require a good attitude to the cold metal forming.

-Al-Cu-Mg alloys are particularly designed and suitable for aerospace and automotive applications, due to their low weight, **good mechanical strength** and excellent corrosion resistance.

-Yield strength, ductility and stress corrosion cracking resistance of 2024 and 2014 are mostly determined by the **strengthening precipitation** occurring during hot deformation or heat treatment

Introduction

-The precipitation sequence for 2014 Al alloys has been extensively investigated .

-In particular, the **ageing response** during elevated temperatures strongly depends on the Cu/Mg ratio .

-The present work focuses on the microstructure investigation of a hot extruded and **warm deformed** 2014+Zr aluminium-copper-Mg alloy.

Material

The 2014 aluminium alloy had the following chemical composition (wt.%): Cu=4.32, Mg=0.49, Zr=0.12, Si=0.68, Fe=0.23, Mn=0.77, Ti=0.03, Al=bal.

-The modified 2014Zr is designed to improve the mechanical properties of the base 2014 Al-Cu-Mg alloy. The role of Zr lies essentially in **inhibiting the recrystallisation** through the precipitation of fine spherical and coherent Al_3Zr particles.

-Small Zr addition promotes a decomposition of the supersaturated solid solution of Al responsible for the formation of a metastable $L1_2$ Al_3Zr phase .

-Consequently, **Al_3Zr particles** are most effective in pinning grain and subgrain boundaries during thermal and mechanical processing .

As received material

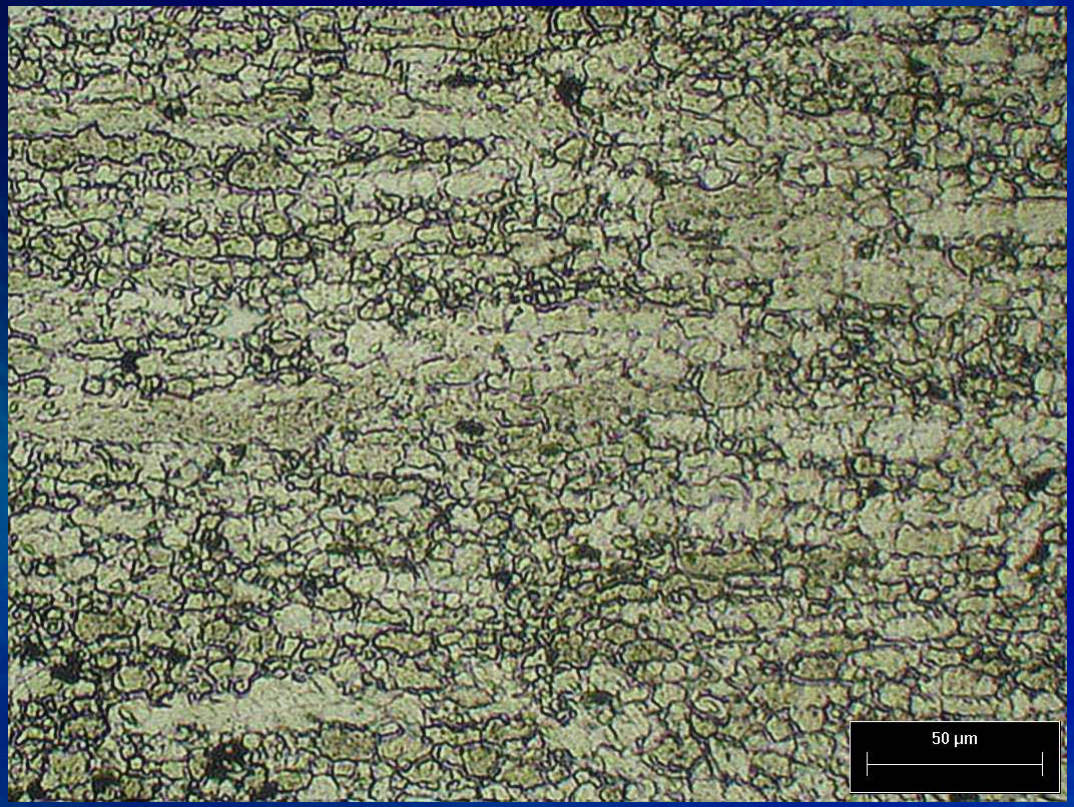

-Specimens for transmission electron microscopy (TEM) were ground to a thickness of about 100 μm, then discs were prepared by means of double-jet electro-polishing with a solution of 1/3 HNO_3 in methanol at –35°C, 20V and a current of 40-50mA/mm^2. .

-TEM thin foils were stored in a vacuum chamber to minimise environmental oxide contamination of the specimens' surface. Investigations were carried out in a Philips CM200 equipped with a double-tilt specimen-holder .

-Two-beam conditions were also used to obtain thickness fringes recording images form constant thickness regions. The volume fraction of the hardening particles was estimated by recording micrographs having (110), (120) and (111) matrix zone axis .

As received material

2 μm

Strengthening due to the **sub-micron grain size** was the largest contribution to alloy strength, followed by **precipitate strengthening** and solid solution strengthening.

The addition of a transition element and in particular the **Zr** one provides, on one hand the **increasing of strength level at room temperature**, and on the other hand the microstructural stability at higher temperatures by forming very fine stable dispersoids.

These dispersoids represent very efficient nuclei for **precipitation of coarse, equilibrium precipitates.**

As received material

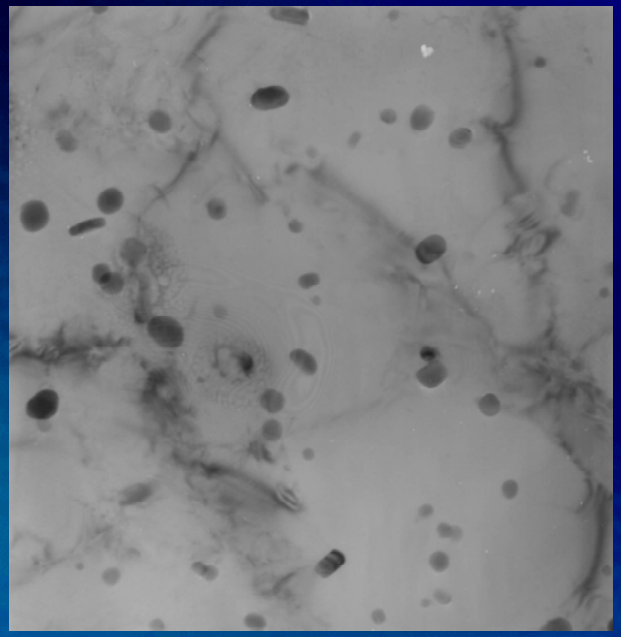

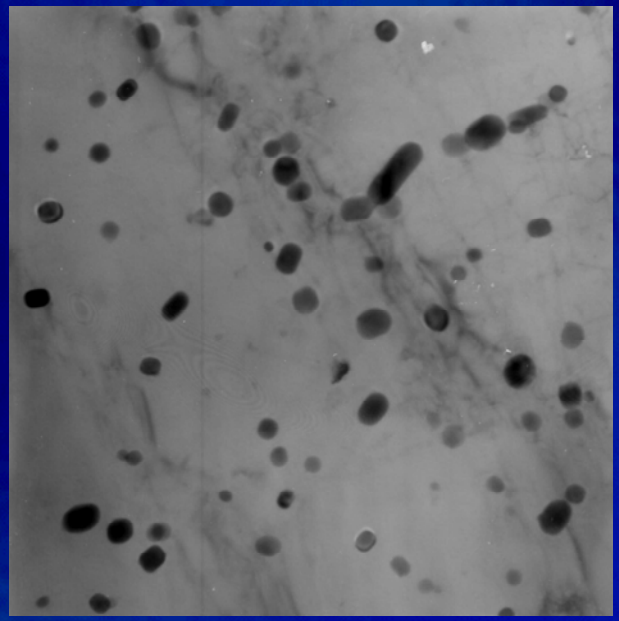

-Al_3Zr precipitates individuated in the Zr modified 2014 aluminium alloy

Workability

One of the most important engineering parameter, during metal working operations, is the workability which describes the **easy with which the material can be shaped** by plastic flow without the onset of fracture.

Workability of metallic materials is strongly influenced by the **processing parameters** such as temperature and strain rate, and all this parameters influence also the **development of microstructures** during formability processes.

Some metalworking processes such as forging are essentially compressive while others such as stretch forming are essentially tensile.

However, during working some stress components can be **compressive or tensile** in the same workpiece.

Usually it is difficult to measure workability because of all the variables which take place during deformation, for this reason a lot of simple laboratory tests have been developed to simulate all the **stress components** in the workpiece during deformation.

The control and design of this processes depend on a large number of parameters such as the material properties of the workpiece, the ambient conditions, the thermomechanical parameters, the mechanics of plastic deformation, the equipment used, etc.

Another important aspect is represented by the friction conditions due to different materials, the worpieces and the die, in contact.

Hot-torsion and hot-compression tests can give a good indication on the possibility to **deform plastically a material** under different conditions of temperature and strain rates.

Torsion tests allow to achieve the **strain levels of most hot and warm metal forming operations** without the limitations imposed by necking in tension tests or by barrelling or friction forces in compression tests, on the other hand, compression tests simulate better than torsion ones the true forming conditions which are present in the die forging.

Torsion tests can be carried out on this kind of materials in order to calculate a lot of mechanical properties such as modulus of elasticity in shear, yield shear strength, ultimate shear strength, modulus of rupture in shear, and ductility.

In torsion test **large strains can be reached** before plastic instability occurs in the material, and all the problems related with friction are eliminated. Torsion testing are carried out by applying, on cylindrical specimens a torsional moment about the longitudinal axis.

The shear stress versus shear strain curve can be determined by measuring the torque and the angle of twist of the tested specimens over a predetermined gage length.

Warm forming tests

-Torsion tests were carried out at the temperatures of 200, 225, 250, 275, 300 °C and strain rate range 10-3-1 s-1.

-The samples were heated using an induction furnace; the temperature stabilisation time was 6 min.

-The gauge section of samples was a solid cylinder with a length (L) of 7 mm, and a radius (R) of 4 mm; the fillet radius between the gauge section and the shoulders was 0.5 mm.

Warm forming tests

-The torque (Γ) and the twist angle (θ) were converted to surface shear stress (τ) and strain (γ) by the relationships:

$$\tau = \frac{\Gamma}{2\pi R^3}(3 + n' + m')$$

$$\varepsilon = \gamma / \sqrt{3}$$

Where n' (=d log Γ/d log θ) is the work hardening rate and m' (=d log Γ/d log θ) is the revolution rate sensitivity coefficient of torque.

Warm forming tests

-Equivalent stresses (σ) and strains (ε) were derived from surface shear stresses and strains by means of the Von Mises yield criterion.

-Because of the temperature increase (ΔT) due to the deformation heating, the flow curves for $\varepsilon \geq 10^{-1}\ s^{-1}$ did not correspond to isothermal conditions. Therefore, a temperature correction was applied to flow stress under such conditions. For each value of equivalent strain, the temperature increase was calculated using the following relationship:

$$\Delta T = \frac{\beta \int_0^{\varepsilon} \sigma d\varepsilon}{\rho c}$$

Warm forming tests

-Where β the deformation heat factor, ρ is the material density, and c is the heat capacity.

-The temperature increase was used to offset flow-softening effects due to the deformation heating by correcting flow stress employing the equation:

$$\sigma_c = \sigma + \Delta\sigma = \sigma + \Delta T \frac{d\sigma}{dT}$$

-where σ_c is the flow stress corrected for the deformation heating.

Warm forming tests

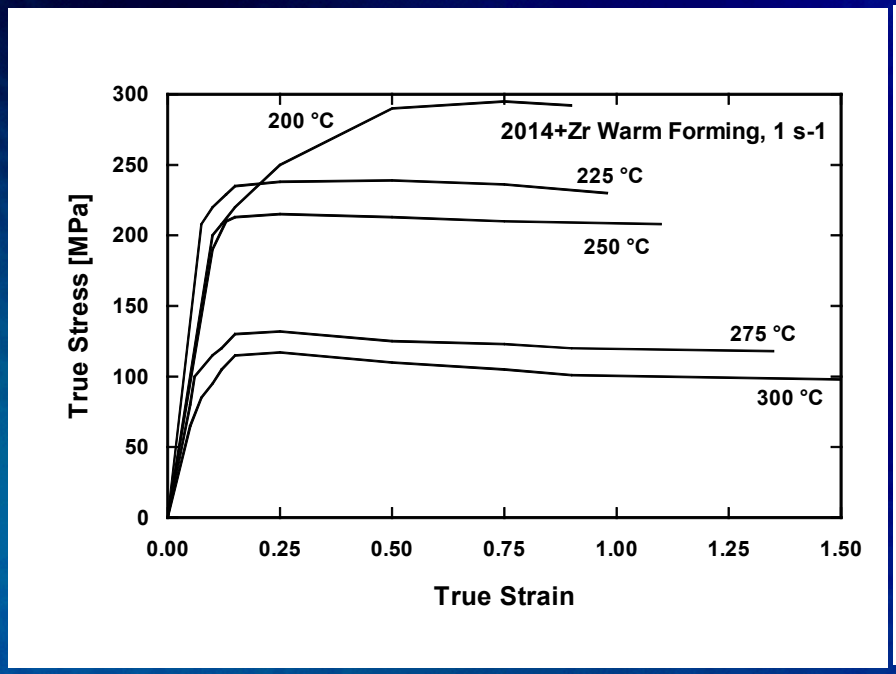

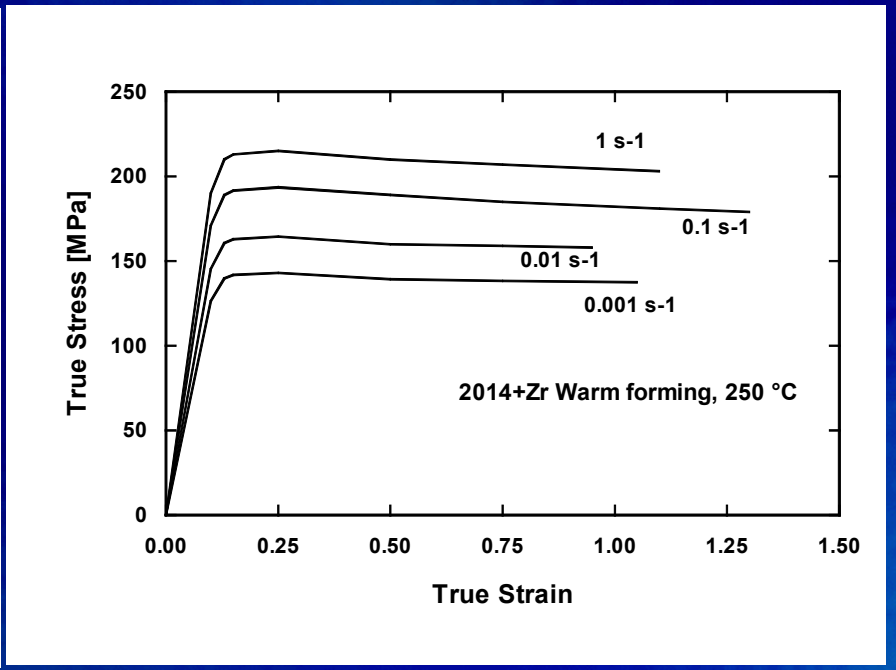

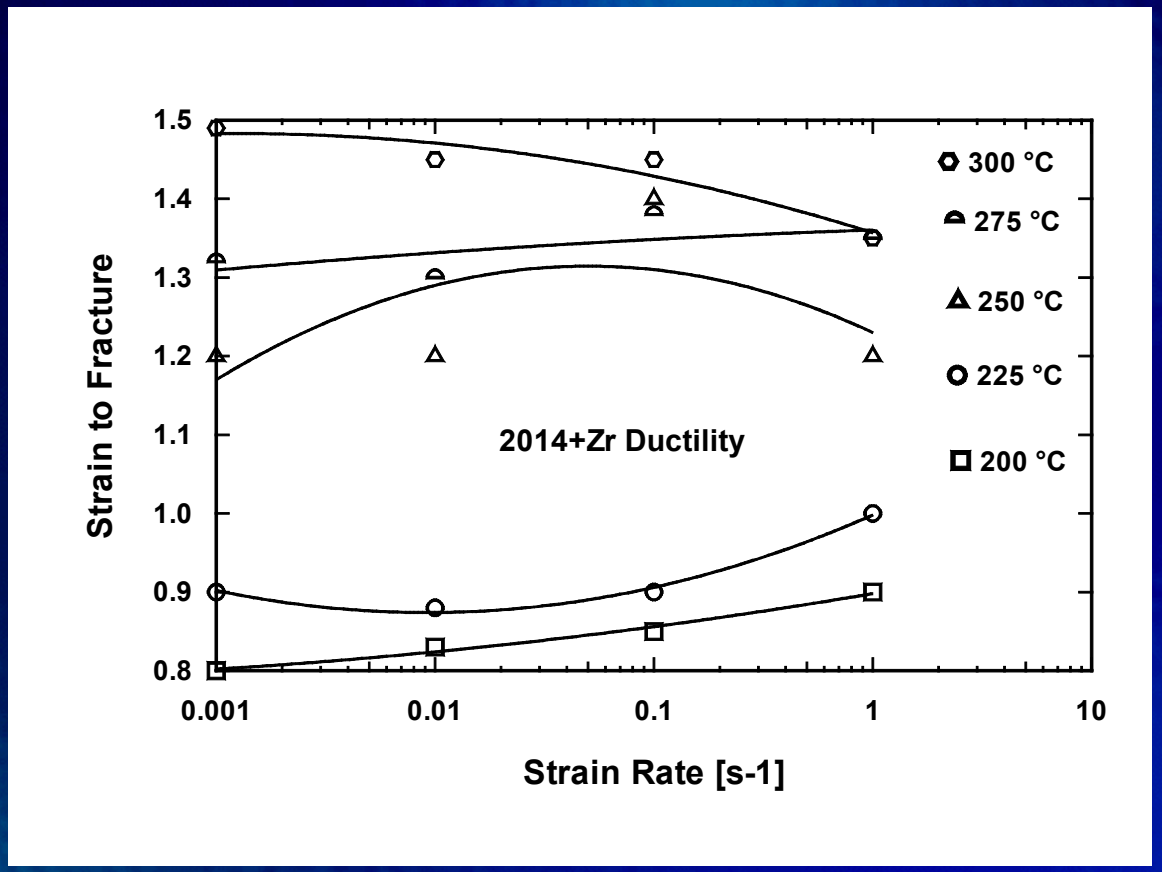

The ductility of the material was calculated as **Strain to fracture vs. Strain rate** for all the temperatures investigated.

The warm forming behaviour of Zr-stabilized 2014 aluminium alloy was subsequently modelled by correlating flow stress to strain rate and temperature according to the well known constitutive equation:

$$Z = \dot{\varepsilon} \cdot \exp\left(\frac{Q}{R \cdot T}\right) = A \cdot \left[\sinh(\alpha \cdot \sigma)\right]^n$$

where Z is the Zener –Hollomon parameter representing the temperature modified strain rate, Q is the activation energy for deformation, R is the universal gas constant, T is the absolute temperature, is the strain rate, A, n and α are material parameters.

The activation energy was calculated by the relationship:

$$Q = -R\left.\frac{\partial \ln \dot{\varepsilon}}{\partial (1/T)}\right|_{\sigma} = 2.3R\left.\frac{\partial \log \dot{\varepsilon}}{\partial \log \sinh(\alpha\sigma)}\right|_{\varepsilon,T}\left.\frac{\partial \log \sinh(\alpha\sigma)}{\partial (1000/T)}\right|_{\varepsilon,\dot{\varepsilon}}$$

The value of the stress multiplier α was calculated by means of an optimisation procedure and $\alpha = 0.014\ (\mathrm{MPa})^{-1}$ gave the best correlation coefficient for the linear relationships and

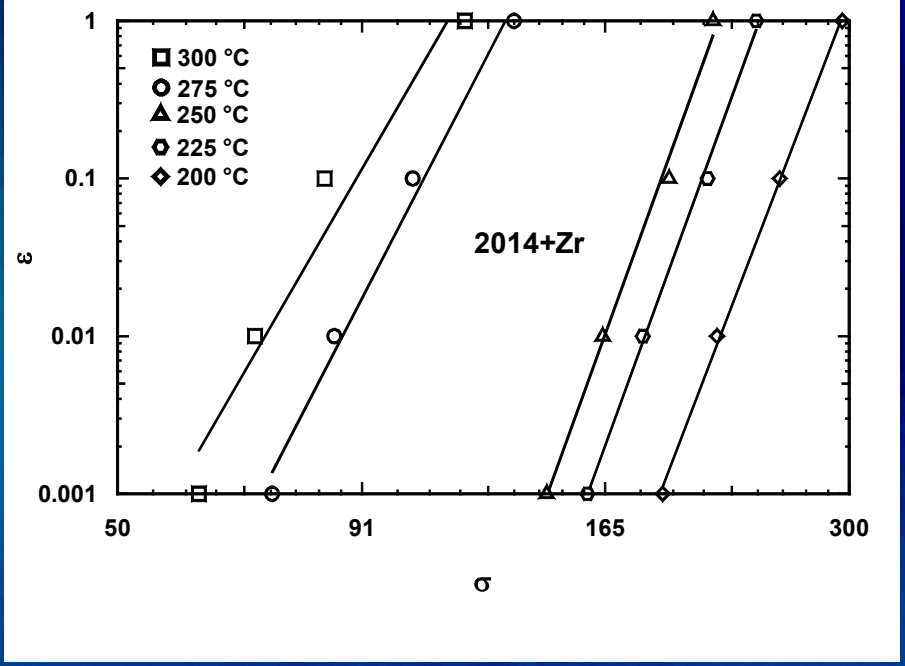

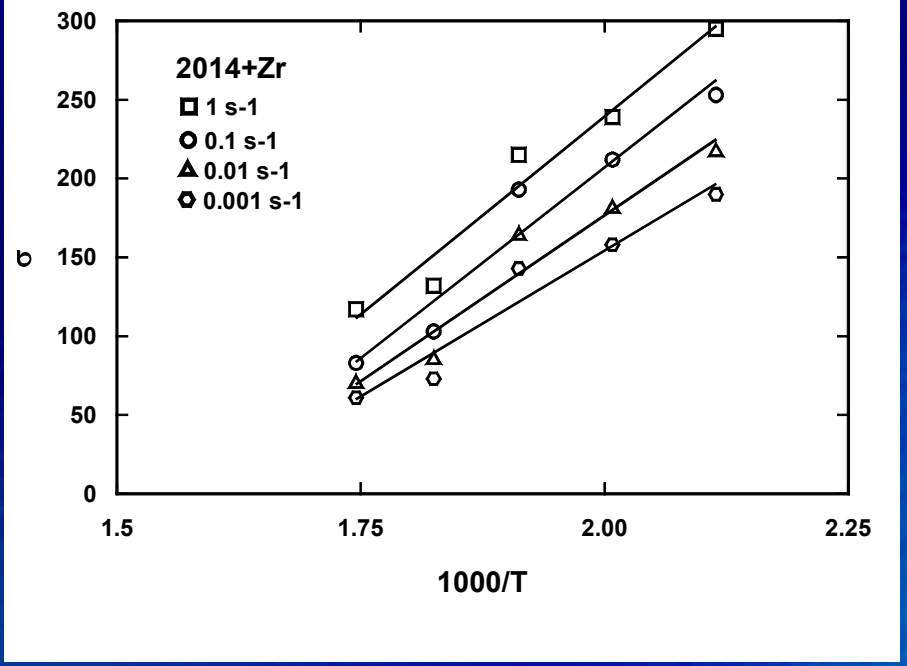

$$Q = -R\left.\frac{\partial \ln \dot{\varepsilon}}{\partial (1/T)}\right|_{\sigma} = 2.3R\left.\frac{\partial \log \dot{\varepsilon}}{\partial \log \sinh(\alpha\sigma)}\right|_{\varepsilon,T}\left.\frac{\partial \log \sinh(\alpha\sigma)}{\partial (1000/T)}\right|_{\varepsilon,\dot{\varepsilon}}$$

The slopes of at constant T and at constant strain rates were calculated, leading to a value of the activation energy of **195 kJ/mol** by using the results from 250 to 300 °C

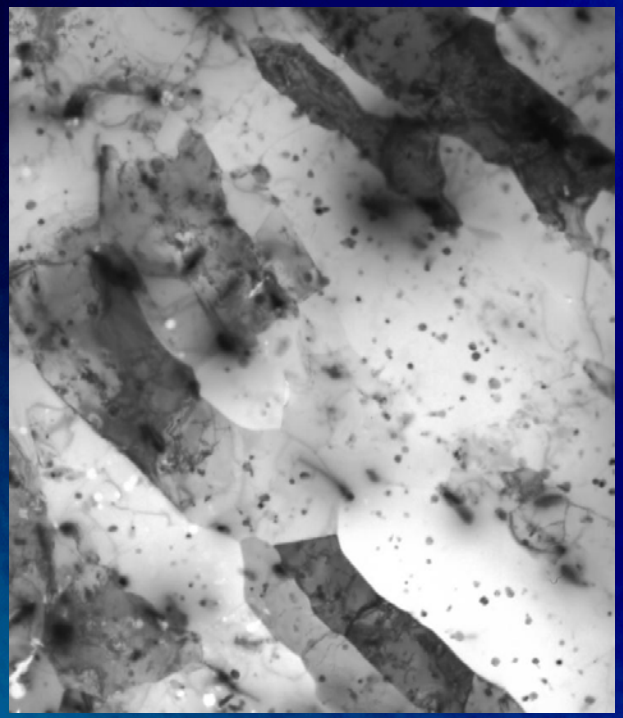

2 μm

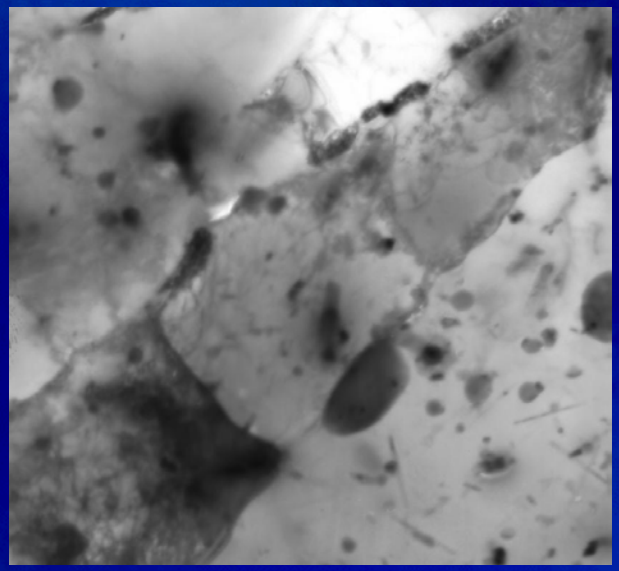

500 nm

TEM micrograph of Zr modified 2014 aluminium alloy torsioned at 250 °C, 10-1 s-1 showing the grain boundary pinning effect of Al_3Zr precipitates.

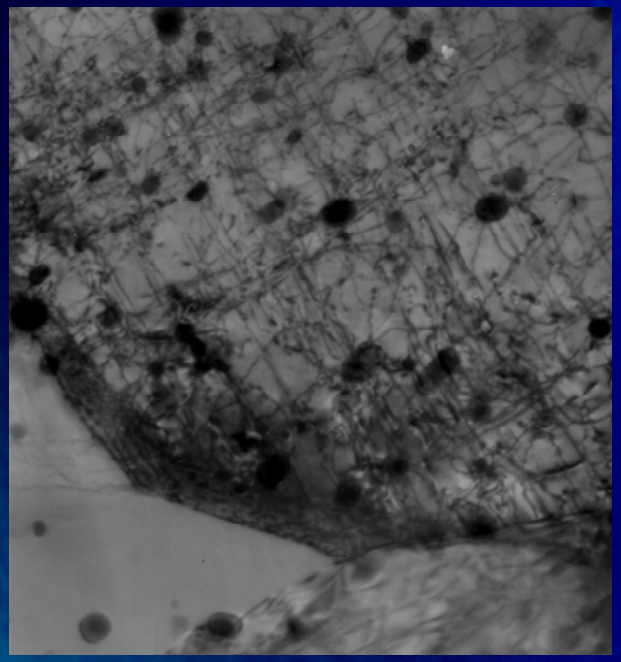

500 nm

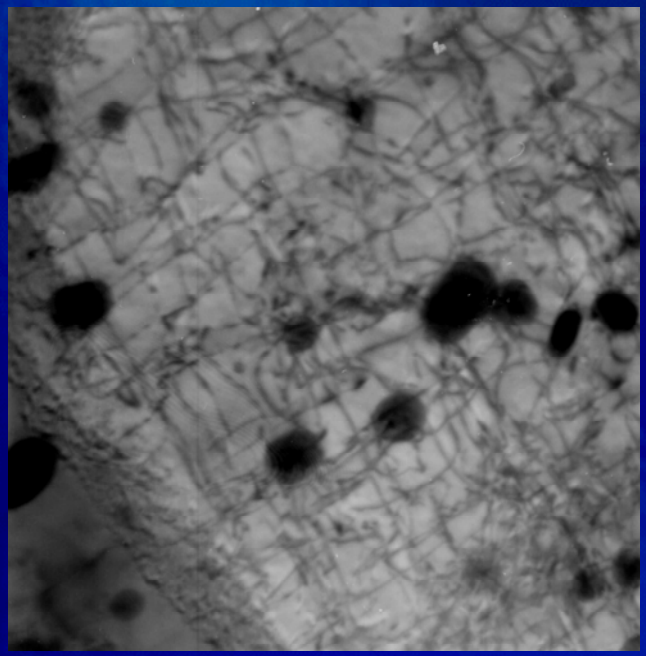

300 nm

TEM micrograph of Zr modified 2014 aluminium alloy torsioned at 250 °C, 10-1 s-1 showing the interaction between precipitates and dislocations.

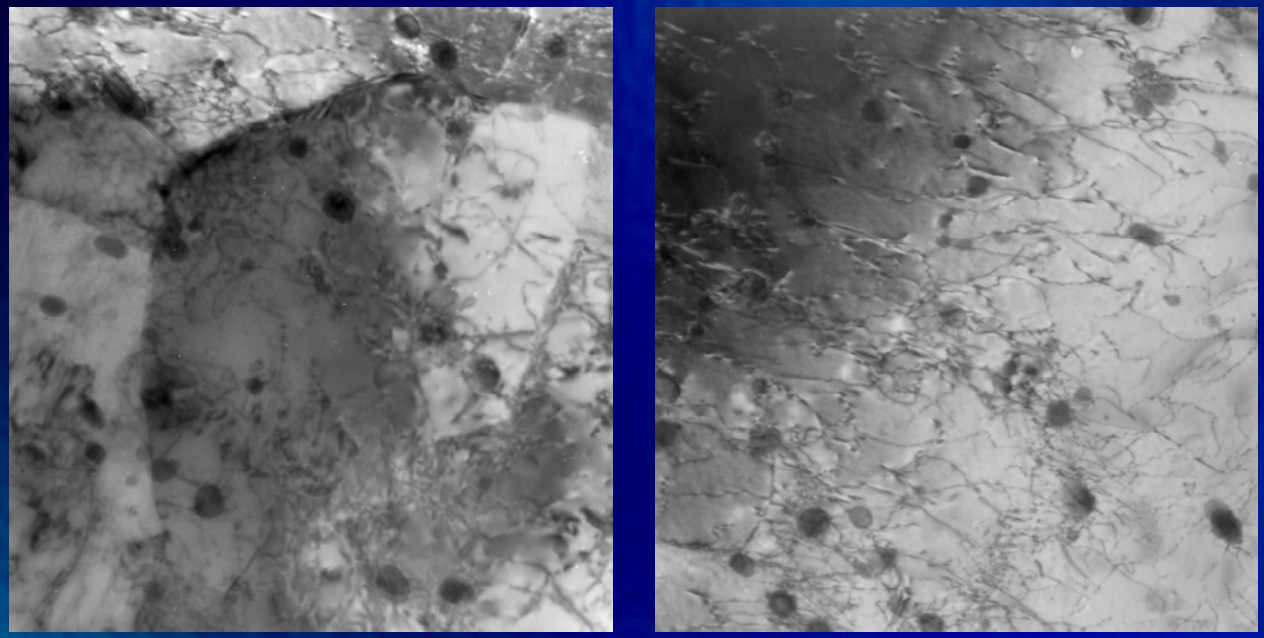

TEM micrograph of Zr modified 2014 aluminium alloy torsioned at 225 °C, 10-1 s-1 showing the interaction between precipitates and dislocations

Introduction

The cyclic fatigue process comprises many macro and microscopic phenomena such as cyclic plastic deformation of the material and damage initiation due to the formation of microscopic cracks which grow and coalesh forming one or more macroscopic cracks that propagating in the material lead to catastrophic failure;

the analysis of fatigue crack growth is a very difficult task to fulfil due to the complexity of the fatigue damage processes involved;

Introduction

Microstructure play an important role in the fatigue crack growth resistance of aluminium alloys controlling the deformation mode and the subsequent crack initiation and propagation behaviour;

the present work is aimed to describe the different behaviour of fatigue micromechanisms of 2014+Zr aluminium alloy.

Fatigue tests

-The cyclic fatigue tests were conducted in the axial total stress-amplitude control mode under fully-reversed, push-pull, tension-compression loading such that the magnitude of negative stress amplitude equals the magnitude of positive one ($R=\sigma_{min}/\sigma_{max}=-1$).

-The fatigue crack growth and propagation of 2014+Zr aluminium alloy has been studied by using a resonant electro-mechanical testing machine (RUMUL) under constant loading control up to 250 Hz sine wave loading.

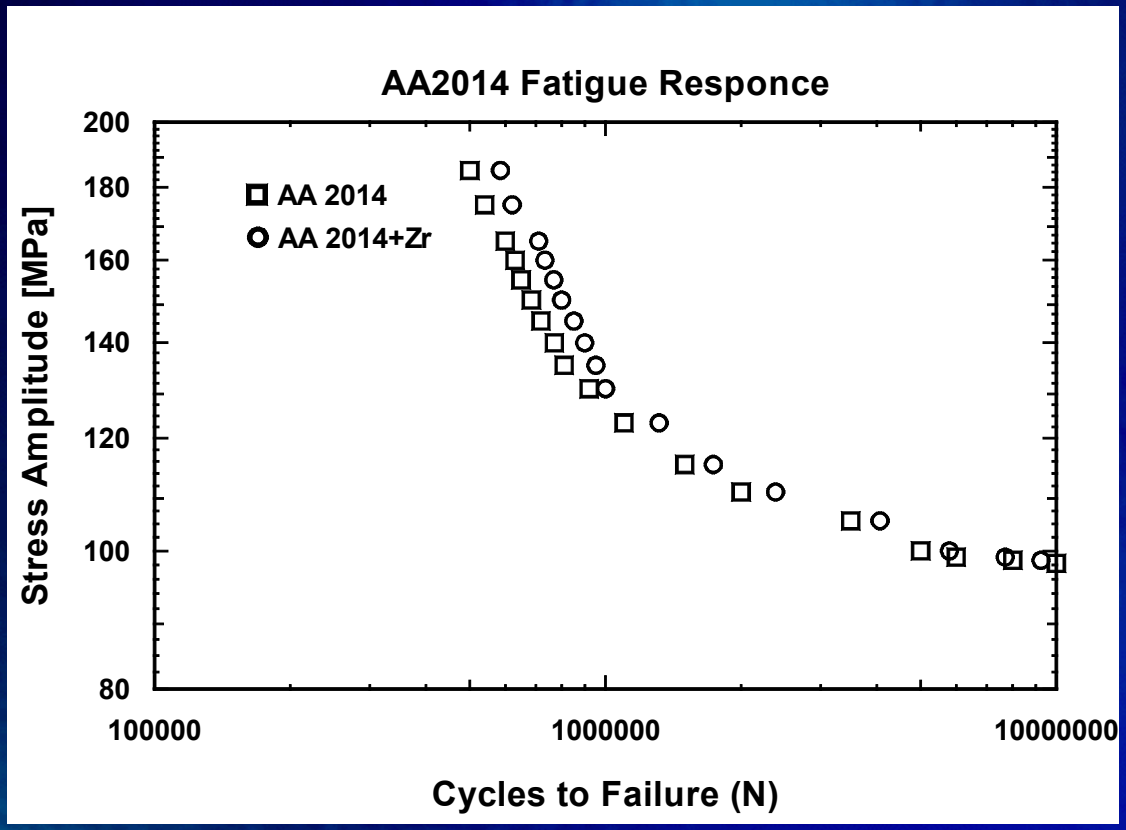

Endurance fatigue curve (S-N) for the AA2014 aluminium alloy in the in the Zr-modified and non modified conditions;

a fatigue life of 10^7 cycles at 110 MPa was recorded in the as received condition while a fatigue life of 10^7 cycles at 100 MPa was recorded for the unstabilized alloy

Fatigue failure is governed, in metallic materials, by nucleation of microcracks which propagate slowly during cyclic deformation until one of them reaches critical dimensions producing catastrophic failure;

Large precipitates are responsible for fatigue crack initiation in commercial aluminium alloys, strain localization occurs in such materials upon cyclic deformation, this result in increasing in dislocation density, large slip offsets on the surface or stress concentration at the grain boundaries, and early fatigue crack initiation by either grain boundaries or inclusion fracture.

The microstructure of the as-received material showed very small equiaxed grains. At higher allowable magnification of the optical microscope coarse- and intermediate-size second phase particles were observed inside the grains and at grain boundaries;

Fracture surfaces of the cyclically deformed fatigue specimens were observed at low magnification in order to identify the zones of fatigue initiation and final failure, at higher magnifications in order to identify the regions of microscopic crack formation and growth and microscopic plastic mechanisms.

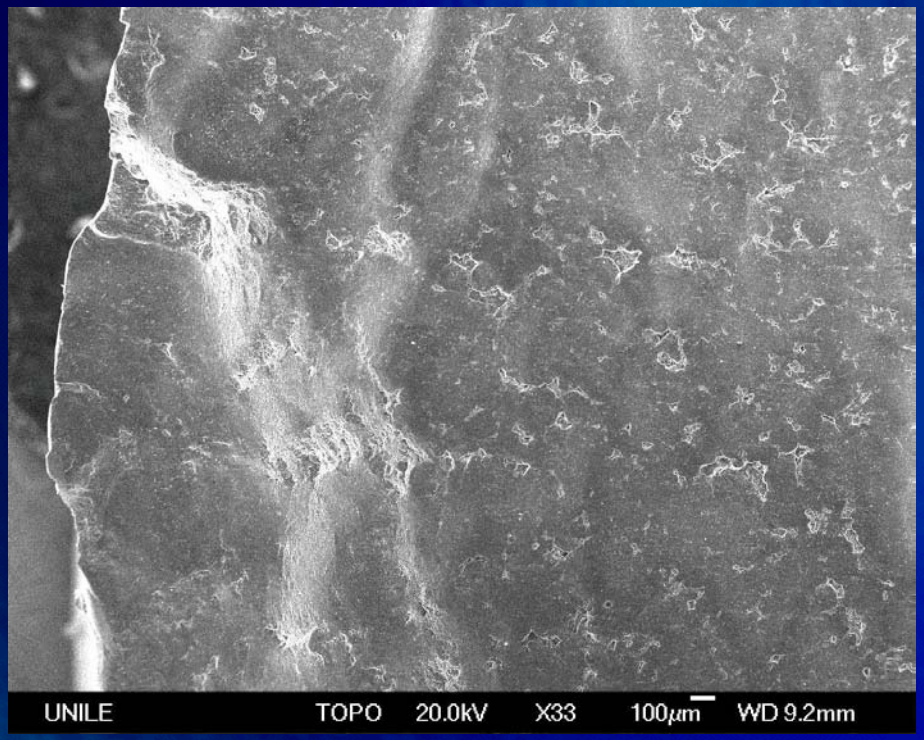

FEGSEM micrographs of the fracture surfaces of Zr-stabilized 2014 aluminium alloy tested at 125 MPa failured after $3.5*10^5$ Cycles.

All the fracture surfaces show distinct regions of stable crack growth and overload, the distance between the two regions is more marked by increasing the cyclic stress

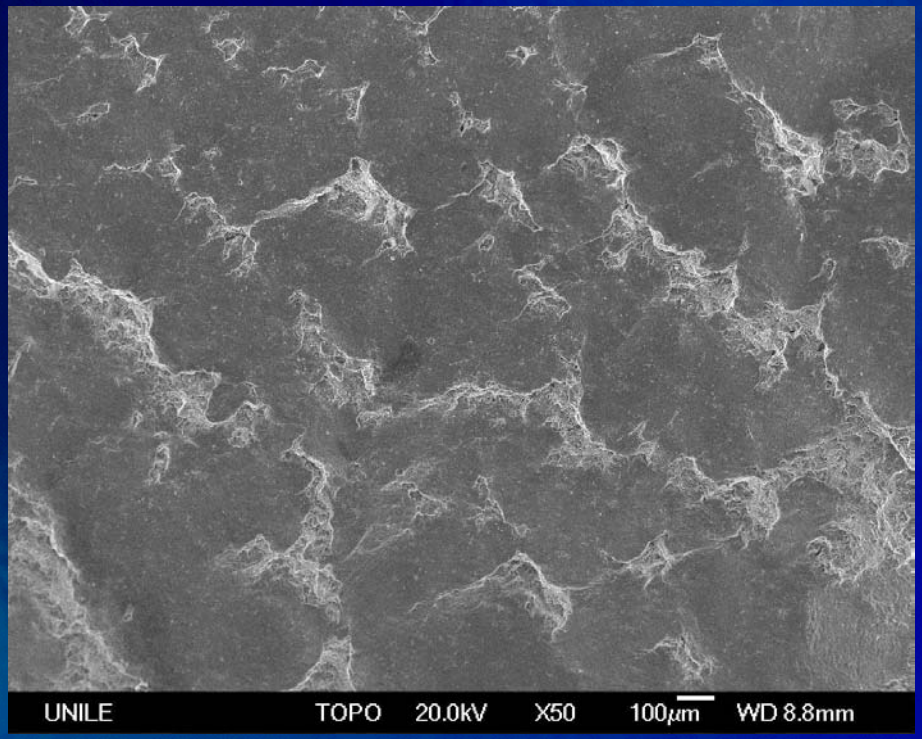

Regions of stable crack growth and overload observed in the Zr-stabilized 2014 aluminium alloy tested at 125 MPa failured after $3.5*10^5$ Cycles

Regions of stable crack growth and overload observed in the Zr-stabilized 2014 aluminium alloy tested at 115 MPa

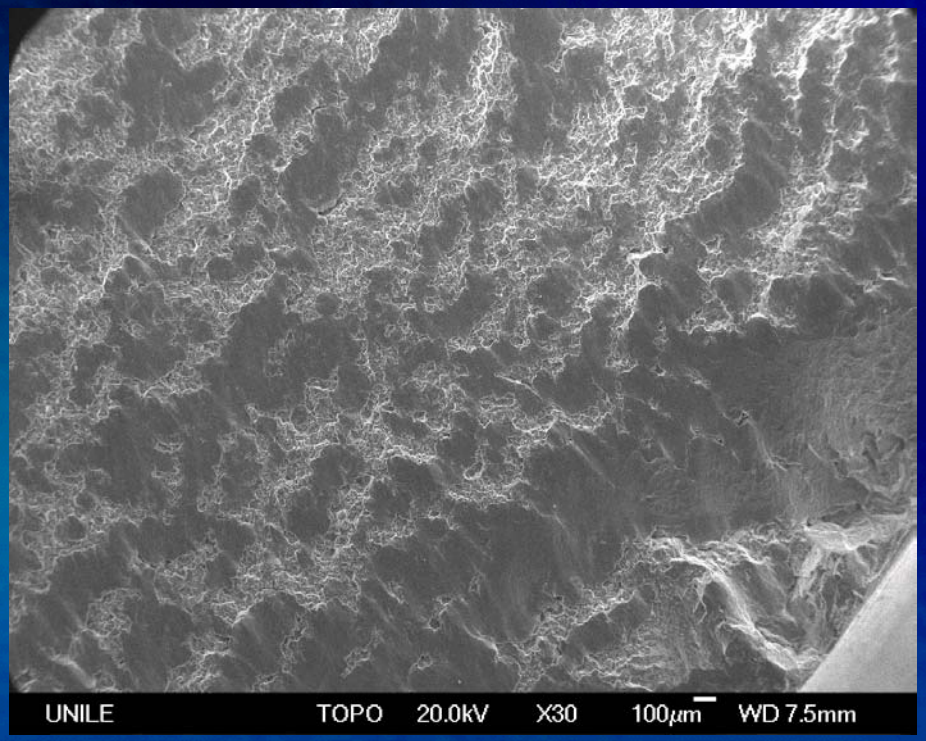

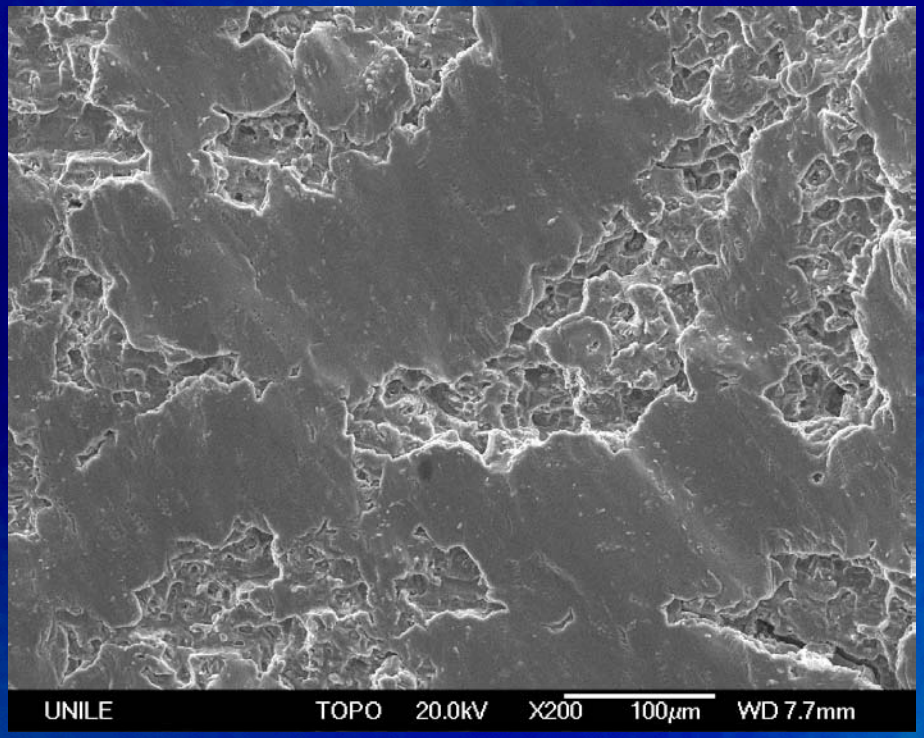

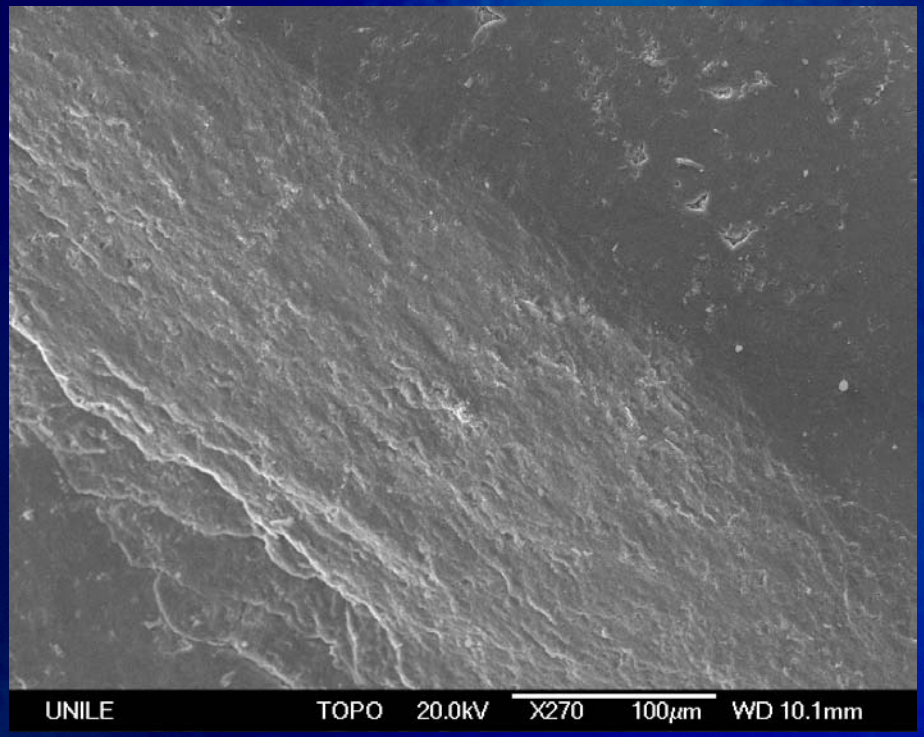

Regions of stable crack growth and overload observed in the Zr-stabilized 2014 aluminium alloy tested at 100 Mpa failured after 10^7 Cycles .

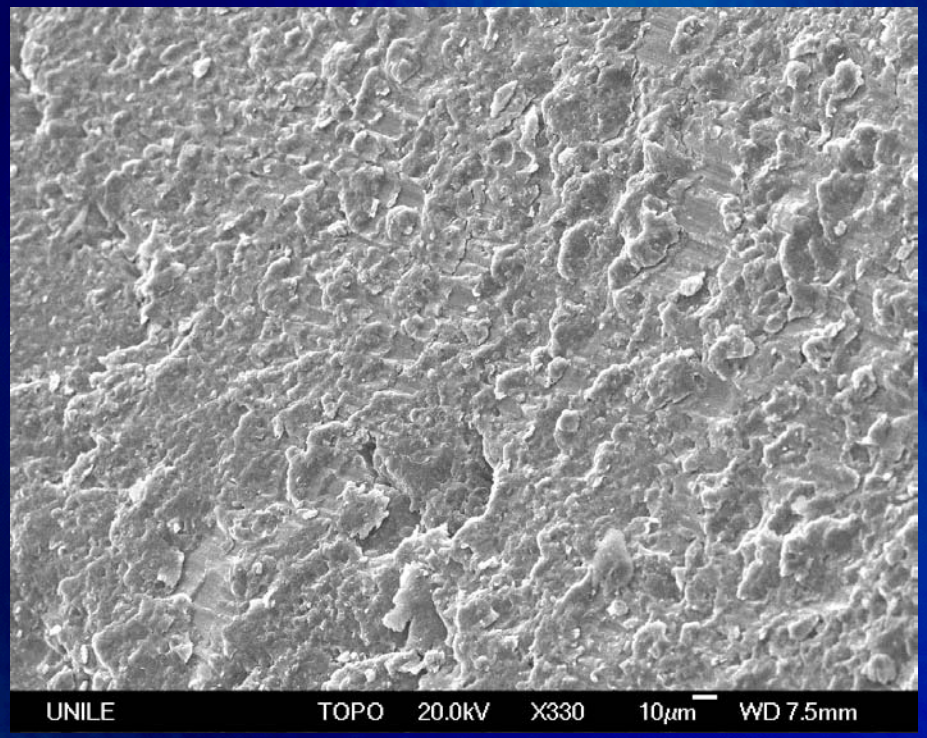

FEGSEM micrographs of the fracture surfaces of Zr-stabilized 2014 aluminium alloy tested at 100 MPa.

In this kind of materials the microcracks formed initially in direction parallel to the principal stress axis, grow and coalesh forming one or more macroscopic cracks that propagate in the same direction leading to the material failure.

During cracks growing, the plastic zone at the crack tip begin to increase and many grains are so involved in the plastic deformation; the crack is able to propagate along different slip planes by simultaneous or alternating shear on two slip systems. This double slip mechanism produces a crack path normal to the load direction producing many fatigue striations. All the FEGSEM observations revealed the presence of the classical fine striations in the regions of stable crack growth, all the evenly spaced striations give the behaviour and the direction of crack propagation in the microstructure and localized microplasticity

These fine spaced striations are proper of the initiation of stable crack growth through the alloy during deformation.

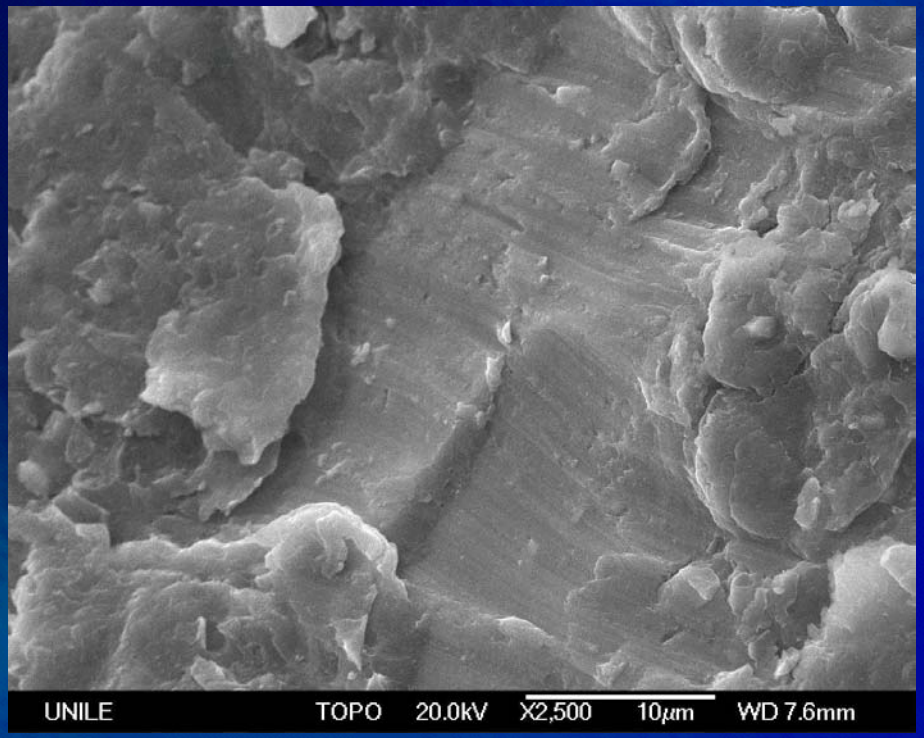

Fine and shallow fatigue striations observed in the region of early crack growth in the specimen tested at 110 MPa

All the crack initiation and growth is normally attributed to the incremental accumulation of microplastic damage of the material, under cyclic loading, at a localized level.

The accumulation of damage at every cycle in the micro sites and the initiation of slip band activity in the grains oriented along the slip direction lead to the nucleation of many microscopic cracks; isolated areas of small voids were recognized in the regions of stable flow and crack growth

The nucleation of voids produce a decrease of the macroscopic response of the material, by continuing deformation, they growth and coalesh as a result of strain localization causing small increments, at every cycle, of crack tip extension.

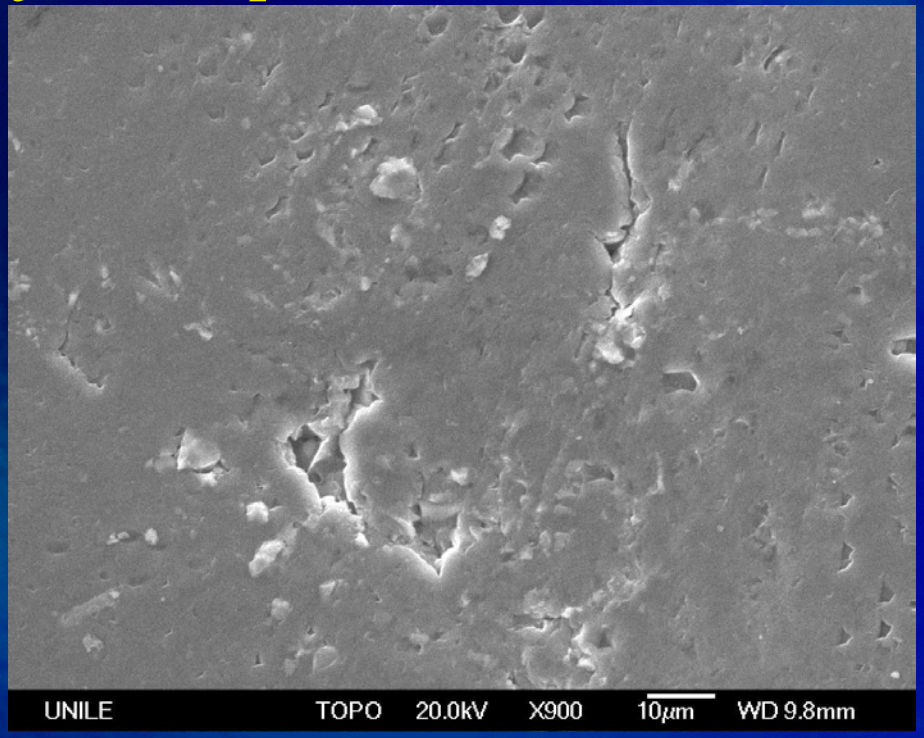

Microscopic cracks observed in the sample tested at 120 MPa

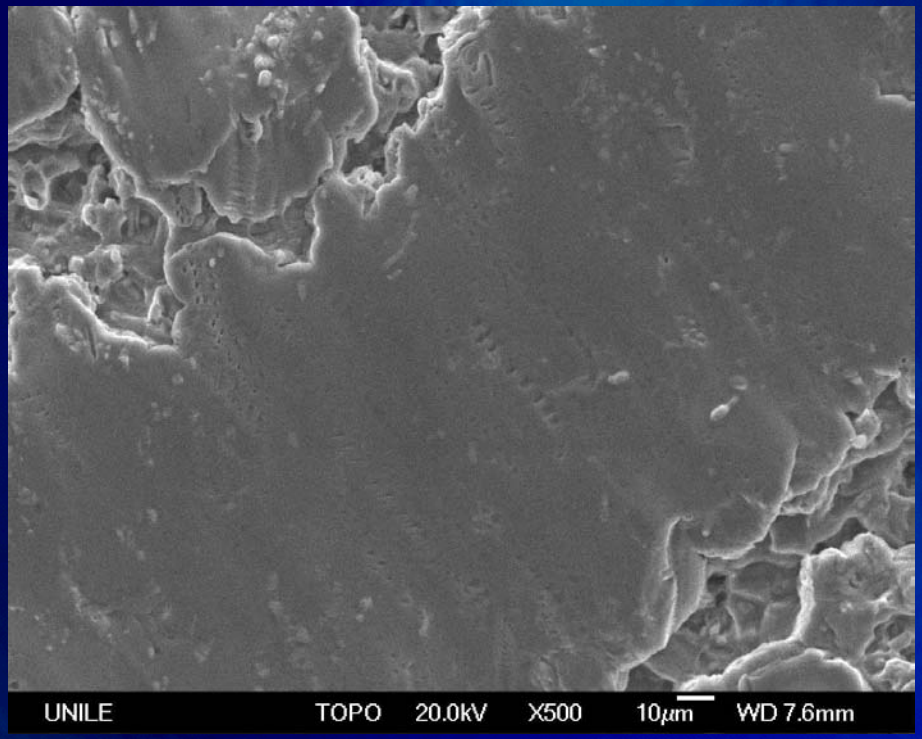

Clam shell formation in the Zr-stabilized 2014 aluminium alloy, specimen tested at 110 MPa.

Conclusions

-The warm forming behaviour of 2014 aluminium alloy stabilized with small Zr additions was studied by employing torsion tests in the temperature and strain rate ranges of 200-300 °C and 10^{-3}-1 s^{-1} respectively;

-The alloy ductility was measured as strain to fracture in all the temperature and strain rate investigated by showing a different behaviour between 250-300 °C and the lower temperatures;

-The activation energy of the material was calculated in warm forming conditions and the Zr effect on microstructural modifications was observed by means of electron microscopy (TEM).

Conclusions

-The response of a Zr stabilized 2014 aluminium alloy to cyclic loading was studied in the present work;

-The cycles to failure at different stress amplitude levels were compared with those obtained for the unstabilized alloy;

-The TEM observation of the modified material showed a very fine subgrain structure characterized by the presence of very fine zirconium trialuminades within the grains, the particles play the role of stabilize the structure, inhibit the recrystallization and increase the strength of the alloy in all the tested conditions.

-Fracture observations were performed by using a scanning electron microscope equipped with field emission gun in order to describe the behaviour of the material during cyclic loading.